Diagnostic and Interventional Imaging (2013) **94**, 1211—1223

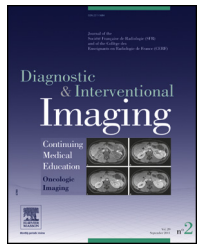

CONTINUING EDUCATION PROGRAM: FOCUS...

Arterial spin labeling (ASL) perfusion: Techniques and clinical use

J.-C. Ferré[a,b,c,d,*], **E. Bannier**[b,c,d], **H. Raoult**[a,b,c,d], **G. Mineur**[a], **B. Carsin-Nicol**[a], **J.-Y. Gauvrit**[a,b,c,d]

[a] *CHU de Rennes, Department of Radiology, Hôpital Pontchaillou, 2, rue Henri-Le-Guilloux, 35033 Rennes cedex 9, France*
[b] *Plateforme Neurinfo, CHU de Rennes, Hôpital Pontchaillou, 2, rue Henri-Le-Guilloux, 35033 Rennes cedex 9, France*
[c] *INRIA, VisAGeS unité/projet U746, 35042 Rennes, France*
[d] *INSERM VisAGeS unité/projet U746, UMR 6074, Irisa, Université Rennes 1, 35043 Rennes cedex, France*

KEYWORDS
MRI;
Perfusion;
Brain;
Kidney

Abstract Arterial spin labeling (ASL) perfusion is a MRI technique to quantify tissue blood flow. ASL is a non-invasive technique that labels the protons in the arterial blood by radiofrequency pulses, without the exogenous injection of contrast media. This article has three goals: 1) present the principles of ASL perfusion, the types of labeling and the ways to obtain the mapping; 2) specify and the quality criteria for the mapping obtained, while emphasizing the artifacts; and 3) describe the main encephalic and renal applications.

The study of tissue perfusion provides functional information about the lesion characterization and the prognosis in a great many disorders. Different techniques are used in everyday clinical practice: the perfusion CT-scan, T2*-weighted perfusion MRI (or dynamic susceptibility contrast MRI: DSC-MRI) and the techniques of nuclear medicine, in particular single-photon emission computed tomography (SPECT) whose clinical use is much easier than positron emission tomography (PET). However, all of these techniques are invasive since they require the exogenous injection of a contrast media or use ionizing radiation (CT-scan and nuclear medicine). Since the early 1990's, a quantitative MRI technique has been developed to study perfusion without contrast media, the arterial spin labeling (ASL) perfusion technique. As an endogenous tracer, ASL uses arterial water protons labeled by radiofrequency pulses. Many technical advances (high field MRI, multichannel coils, parallel imaging in particular) have contributed to the development of this technique

* Corresponding author. CHU de Rennes, Department of Radiology, Hôpital Pontchaillou, 2, rue Henri-Le-Guilloux, 35033 Rennes cedex 9, France.
E-mail address: jean-christophe.ferre@chu-rennes.fr (J.-C. Ferré).

2211-5684/$ — see front matter
http://dx.doi.org/10.1016/j.diii.2013.06.010

by limiting the main disadvantage: a low signal-to-noise ratio (SNR). Therefore, ASL reveals, in an entirely non-invasive manner, perfusion anomalies in many disorders, in particular encephalic diseases. ASL sequences have recently become available in clinical MRI scanners. However, their use in everyday clinical practice remains confidential.

This article aims at presenting the principles of ASL, the conditions for its use with clinical MRI scanners and the main artifacts as regards clinical use. Although ASL has been successfully used to study renal perfusion, this article is focused on the study of cerebral perfusion.

Principle of arterial spin labeling perfusion

General principle of arterial spin labeling

It consists of a differential technique during which two acquisitions are carried out: one with the labeling of arterial protons and a control acquisition. With the techniques most often used, the magnetic labeling of arterial protons is carried out upstream from the volume of interest, at the neck vessels, by radiofrequency pulses. The labeled protons then migrate via the arterial vessels towards the brain tissue where they pass from the capillary compartment to the extravascular compartment. At time TI (inversion time) after the pulsed labeling, corresponding to the time required for the labeled protons to perfuse the tissue, the images are acquired with a rapid imaging technique (Fig. 1).

The control acquisition is obtained without arterial labeling. The arterial protons of the volume of interest are then in equilibrium and completely relaxed. The subtraction of the labeled and control acquisitions suppresses the signal from the static tissue and provides a perfusion-weighted image [1]. The difference in signal is only several percent. Many repetitions of labeled-controlled paired images have to be acquired, and averaged to ensure an adequate SNR.

Under several conditions, a perfusion quantification model may be used to obtain the quantitative mapping of the cerebral blood flow (CBF) in mL/100 g tissue/min (Fig. 2).

Main methods for data acquisition

The acquisition of data involves two basic steps: the labeling of the circulating blood protons and the acquisition of images.

Proton labeling techniques

There are three main techniques of proton labeling: continuous labeling (CASL), pulsed labeling (PASL), and pseudo-continuous labeling (pCASL).

Continuous labeling

CASL is the method initially proposed by Williams et al. in 1992 [1,2]. The labeling is continuous through a thin slice at the neck level. The inversion of the magnetization is obtained by the joint application of continuous pulsed radiofrequency for 2 to 4 seconds and a magnetic field gradient in the direction of the flow. Although CASL provides higher perfusion contrast than other types of labeling [3], it has two major disadvantages: the considerable magnetization transfer (MT) effects and the high level of the energy deposited in the tissue (SAR). The MT effects correspond to the partial saturation of macromolecules and a reduction in the signal from the free-water in the studied volume. Several methods have been developed to reduced these MT effects; first for single slice acquisitions and second for multi-slice acquisitions. Their principle is based on the application of additional pulsed radiofrequencies during the control acquisition, although at the price of a high SAR [4]. This effect can be avoided by using labeling-specific coils differing from the image acquisition coil [5,6].

Pseudo-continuous labeling

To limit the duration of the application of the radiofrequency pulse, the CASL may be approached by the use of several RF pulses, using the body coil. This method called ''pseudo-continuous ASL'' has the combined advantages of CASL and PASL [7].

Pulsed labeling

PASL techniques use very short radiofrequency pulses over large labeling zones. There are two groups of PASL sequences

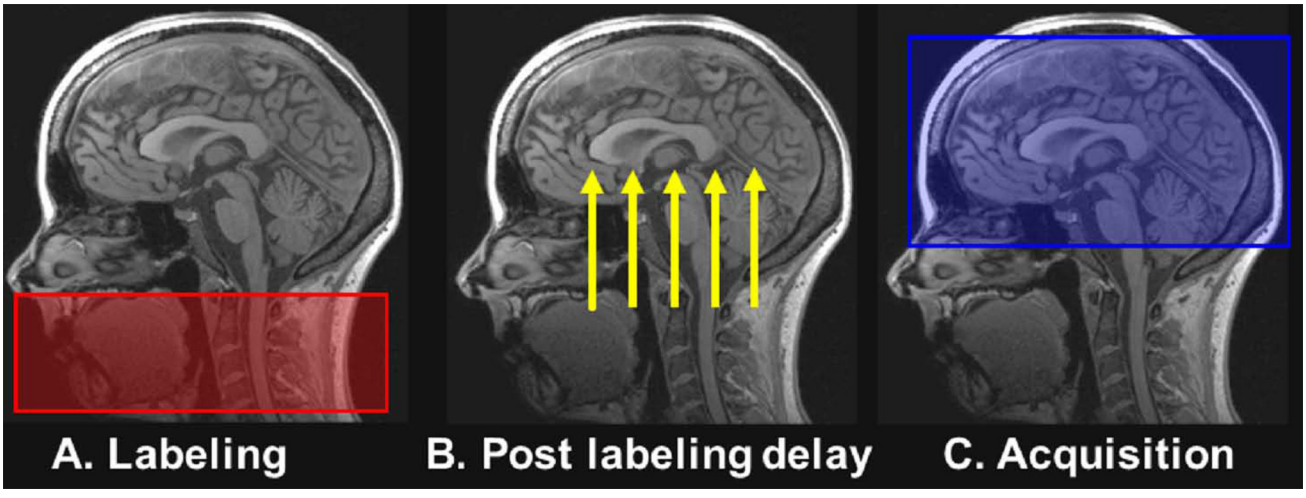

Figure 1. Principle for arterial spin labeling acquisition. Examples of asymmetrical pulsed arterial spin labeling sequences such as PICORE Q2TIPS or STAR.

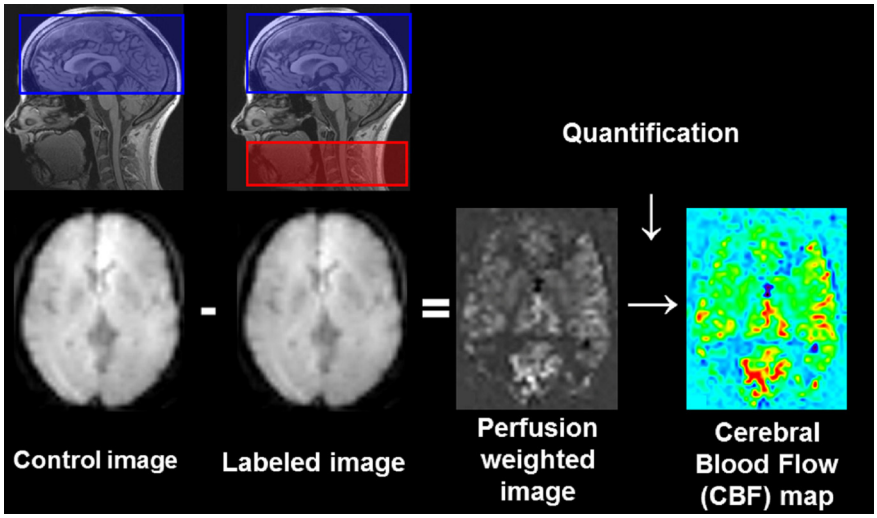

Figure 2. General principle of arterial spin labeling.

that differ according to the zone of labeling with respect to the slices: symmetrical methods and asymmetrical methods [8]. The basic symmetrical method, flow alternating inversion recovery (FAIR), uses a non-selective inversion pulse during the control, that becomes selective with the addition of a slice selection gradient for the labeling [9]. The asymmetrical methods, for which the first version, echo-planar MR imaging and signal targeting with alternative radio frequency (EPISTAR) was described in 1994, have a labeling zone with a thickness of 10—15 mm, located upstream from the volume of interest [10]. With the EPISTAR sequence, an inversion pulse provides the labeling after saturation of the magnetization. During the control acquisition, the labeling volume is located downstream from the volume of interest in order to control the MT effects. Several modifications were then made in this sequence for the multi-slice study [11], while limiting the MT effects (TILT sequence) [12], to improve the profile of the labeling slice (PICORE sequence) [13] and to reduce the sensitivity of the arterial transit time (QUIPPS, QUIPPS II, Q2TIPS sequences) [14,15].

Other methods

Several approaches have also been developed to obtain the selective labeling of an artery to study its downstream territory [16—18], or to selectively label some arterial velocities [19].

Image acquisition

The labeling effect of ASL is weak. Many repetitions of labeled-controlled paired images have to be acquired, and averaged to ensure adequate SNR. Due to its satisfying SNR and the rapid acquisition limiting the movement artifacts, ''echo-planar imaging'' (EPI) is the technique mainly used. The main disadvantage is the presence of distortions in the regions with a high magnetic susceptibility.

3D sequences have been developed to improve the quality of the images. It is possible to use ultra-fast, single-shot 3D sequences combining gradient echo and spin-echo acquisition (GRASE) [20]. Its use thereby facilitates the elimination of the signal from static tissue [21]. This type of sequence theoretically provides a better SNR, a better cover and fewer magnetic susceptibility artifacts than 2D EPI sequences.

Optimization with the clinical MRI scanner

Influence of the MRI hardware

High magnetic field

The use of high magnetic field MRI significantly improves the quality of ASL images [22]. In fact, with high magnetic field, there is a higher increase in signal than in noise and therefore an increase in the SNR. In addition, the lengthening of the T1 of tissue and therefore the proton labeling time in ASL helps increase the perfusion signal. The doubling of the signal in CASL and PASL acquisitions was thereby obtained at 3 and 4 T when compared with acquisitions at 1.5 T [3,23].

Phased array coil

Another approach to improve the SNR of ASL is the use of phased array coils. Due to the sensitivity of the elements at the surface of the coil, the SNR is increased not only in the regions close to the coil, such as the cortex, but also in the entire image [24]. The absolute quantification of the CBF is not affected by the effects of the sensitivity profile of the coil [25]. Thereby, the SNR increases with the number of coil elements [26,27]. In addition, this type of coil enables the use of parallel imaging (PI). PI techniques such as sensitivity encoding (SENSE) or generalized autocalibrating partially parallel acquisitions (GRAPPA) have shown to improve the quality of images [27]. This improvement is especially distinct in long echo train sequences such as EPI. The possible reduction of the TE mainly reduces the magnetic susceptibility artifacts [28].

Data processing and quantification

Application of a model that takes into account the labeling type and parameters is necessary to quantify tissue perfusion from the perfusion-weighted image.

Data pre-processing

Before quantification, the data should be pre-processed to improve the quality of the images. The ASL image series have to be adjusted to correct the subject's movements. They may also be ''denoised'' using the high-resolution anatomical image (3D T1) segmentation [29]. The pre-processing methods used are mainly generic methods. However, the processing of ASL data also requires specific developments. Automatic analysis was proposed to study muscle perfusion by ASL with automatic rejection of images during the detection of considerable movement and with the search for characteristic pixels of vessels by a cluster analysis [30]. Moreover, automatic detection methods for brain vessels, using explicit models, have been developed to facilitate their elimination during multi-TI acquisitions [31]. Asllani et al. have also proposed, for the correction of partial volume effects in the quantification of the CBF, an algorithm that regulates the quantification according to the white matter – grey matter distribution in the voxel [32]. Moreover, Wells et al. have used several ASL de-noising methods. They demonstrated that different methods, in particular analysis by independent components, may reduce errors in the estimate of the CBF and the arterial transit time (ATT) without a modification in image contrast [33].

Quantification

The subtraction between labeled images and control images provides a perfusion-weighted image ($\triangle M$). The relationship between $\triangle M$ and the CBF depends on the proton density of the tissue, the relaxation time T1 of the labeled tissue and blood, as well as their difference. It also depends on the transit time between the labeling area and the volume of interest.

The first model proposed to quantify the CBF was based on several hypotheses: the blood is considered to arrive at a constant speed and the labeled protons are considered to be a diffusible tracer that passes into the tissue as soon as they arrive [1,2]. Therefore, it was possible to use a single compartment model in which the relaxation time of the labeled protons is no longer that of the labeled blood but that of the labeled tissue. Several improvements were then successively proposed to reach the general kinetics model proposed by Buxton et al. [34]. In this model, the difference in magnetization between the labeled and control images is described by using a convolution:

$$\triangle M = 2 \cdot M_{a,0} \cdot \mathrm{CBF} \cdot \int_0^t c(\tau) \cdot r(t-\tau) \cdot m(t-\tau)\, d\tau \qquad (1)$$

where M_0, is the magnetization at equilibrium in an arterial blood voxel, *c(t)* the fractionated arterial input function, *r(t-τ)* the output of the labeled protons from the voxel and *m(t-τ)* the effects of longitudinal relaxation.

This model is applicable with CASL and PASL provided that the parameters are adapted. However, there are many sources of quantification error: the transit time, the vascular artifacts, the form and efficacy of the inversion pulse, the effect of the dispersion of the bolus, the blood-tissue distribution coefficient of the labeled protons and the magnetization of the blood at equilibrium [35].

In addition to the CBF, other perfusion parameters may be estimated with ASL, provided that specific methods of acquisition or different quantification models are used. It is therefore possible to quantify the arterial arrival time (AAT) and the volume of arterial blood with a multi-TI sequence, such as the quantitative STAR labeling of arterial regions (QUASAR) sequence [36].

Arterial spin labeling quality criteria

Table 1 sums up the recommended conditions of acquisition to ensure optimum quality of the mapping obtained. The quality of the mapping obtained in ASL may be altered by several types of artifacts, whether or not specific to the technique or patient-related.

Arterial spin labeling-specific artifacts

Vascular artifacts

Vascular artifacts are mainly visible with PASL, although they may also be visible with CASL. They correspond to hypersignals located in the vascular, arterial or venous, deep or juxtacortical structures. The linear arterial juxtacortical hypersignals should be differentiated from cortical perfusion (Fig. 3). These artifacts are related to the presence of

Table 1 How to optimize the quality of ASL mapping?

Magnetic field	3 T > 1.5 T
Reception coil	Multi-element coil superior to the bird cage coil
Type of labeling	According to indication and magnetic field: PCASL > PASL > CASL[a] With crushers[b]
Acquisition of images	3D superior to 2D
	With elimination of the signal from static tissue, parallel imaging
TE	As short as possible
TR	Sufficiently long for sufficient relaxation of the labeled protons between the acquisitions (TR > 3000 ms)
TI	Sufficiently long to give enough time for the labeled protons to reach the capillaries but sufficiently short to avoid excess relaxation of the labeled protons A great many factors intervene (magnetic field, type of labeling, location of the labeling box, saturation...)

ASL: arterial spin labeling; PCASL: pseudo-continuous labeling; PASL: pulsed labeling; CASL: continuous labeling.
[a] Multi TI is currently not available on clinical machines.
[b] Bipolar gradients applied during the acquisition to eliminate the intravascular signal.

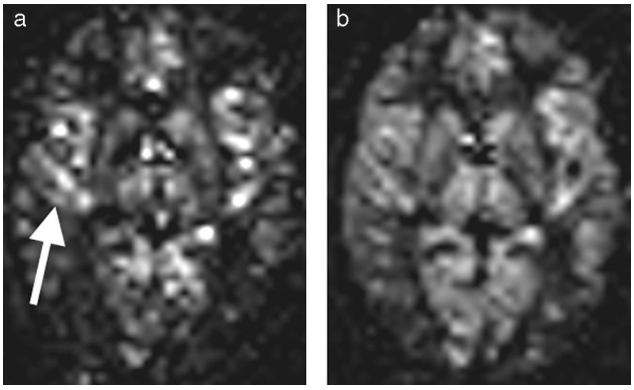

Figure 3. Arterial artifacts. a: the arterial artifacts are visible in the form of hypersignals in the anterior interhemispheric and lateral sulcus (arrow) with a TI of 1200 ms; b: with a TI of 1700 ms, these artifacts are reduced and the parenchymatous signal increases.

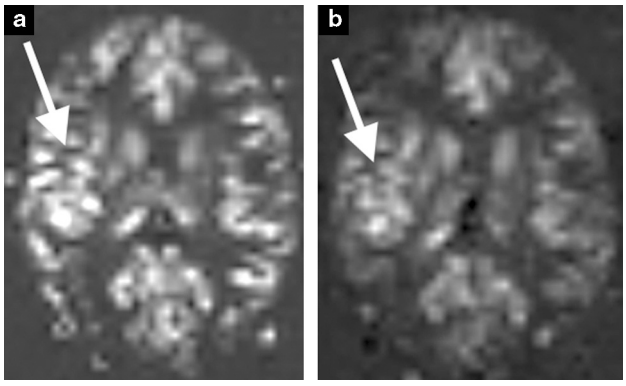

Figure 5. Effect of the application of crushers. a: vascular artifacts (arrows); b: there is a major reduction in these artifacts when bipolar crusher gradients are applied.

labeled protons in the vessels. In the arteries, their presence is often related to the arterial transit time. For example, if the TI chosen is too short, of if the arterial transit time is high, as in severe carotid stenosis, the labeled blood will not have the time to reach the capillaries and will thereby be detected in the arteries (Fig. 4). This artifact may be of clinical value since, for example, it is an indicator of presence and intensity of the collateral arterial network in moyamoya disease [37].

One way to reduce the signal from the vessels in a homogenous manner is to add crushers. They are bipolar gradients applied in several directions during the acquisition, just before the acquisition of images, to eliminate the rapid flow (over several cms/s) (Fig. 5) [38,39].

Venous artifacts are visible with long TI or with certain types of labeling such as the FAIR technique [40].

Signal loss in the upper slices

The overall loss of signal in the upper slices is induced by the relaxation of labeled protons over time. This artifact is especially visible in the upper slices with a caudocranial 2D acquisition. It is above all visible at 1.5 T, since the labeling duration is shorter due to the shorter T1 of the blood (Fig. 6). 3D acquisition reduces this artifact as does the use of parallel imaging that may reduce the time of acquisition of slices, therefore the time between the slices [25].

Physiological hyperperfusion/hypoperfusion

Areas of hypoperfusion and hyperperfusion are sometimes visible in the normal perfusion mapping and are related to physiological modifications in the perfusion.

Areas of hyperperfusion

Visible in the occipital region, according to certain authors, they are due to an activation of the visual areas in the MRI environment [41]. The hyperperfusion visible in the internal frontal region has already been described with other perfusion techniques [42]. This may also involve phenomena related to the transit time and residual vascular signal (Fig. 7).

This aspect is considered as normal in the young and middle-aged subject and decreases with age and the factors of cardiovascular risk [41,42].

Areas of hypoperfusion

These areas extend from the frontal and occipital horns to the frontal and parieto-occipital cortex [43]. They globally correspond to the arterial border-zones (Fig. 8). This hypoperfusion is bound along the TTA of these regions [43]. This aspect may be associated with the difficulty, in some situations, of obtaining a reliable CBF measurement in the white matter [44].

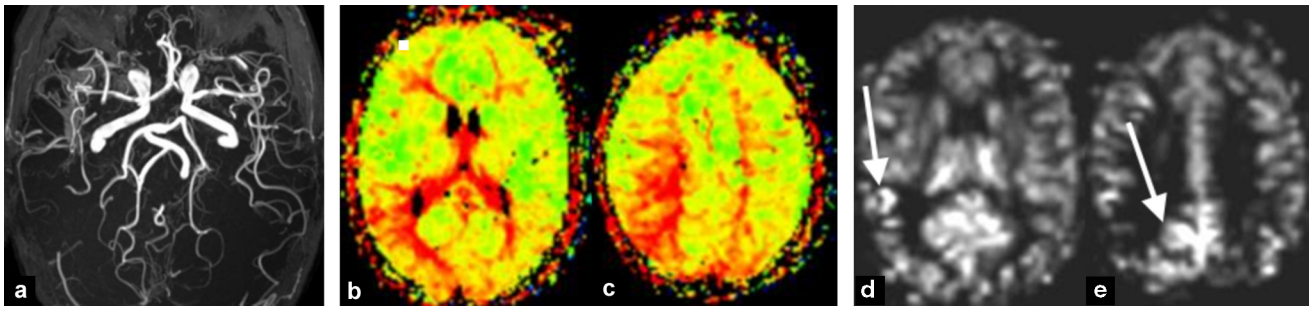

Figure 4. Arterial artifacts, effect of the arterial transit time. a: patient presenting a vasospasm following a subarachnoid hemorrhage, visible on the 3D TOF sequence; b—c: the increase in the time of circulation in the middle, posterior and right posterior junctional brain areas resulting in an increase in the mean transit time on the magnetic susceptibility perfusion mapping; d—e: the same mechanism accounts for the visualization of the arterial artifacts (arrows) and the reduction of the perfusion signal in pulsed labeling.

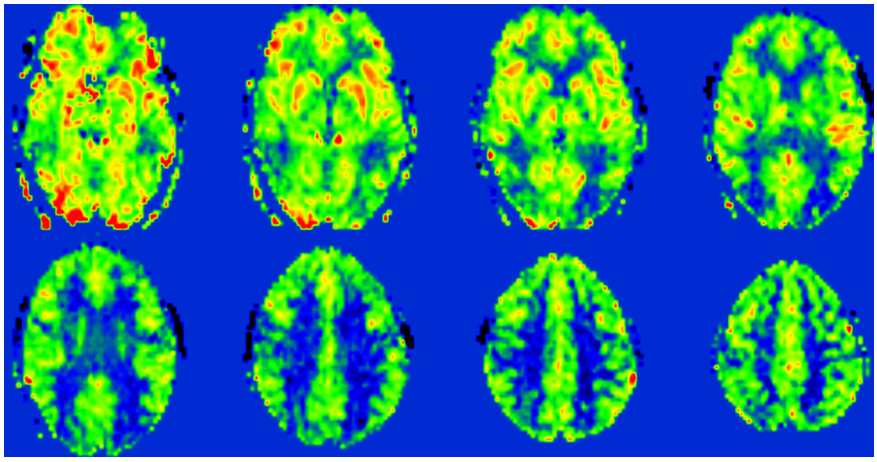

Figure 6. Loss of signal from the upper slices. These arterial spin labeling mappings demonstrate the progressive reduction in signal on the slices acquired later and later. This effect is less distinct at 3 T although still present, and improved with a 3D acquisition and when the TE may be reduced by parallel imaging.

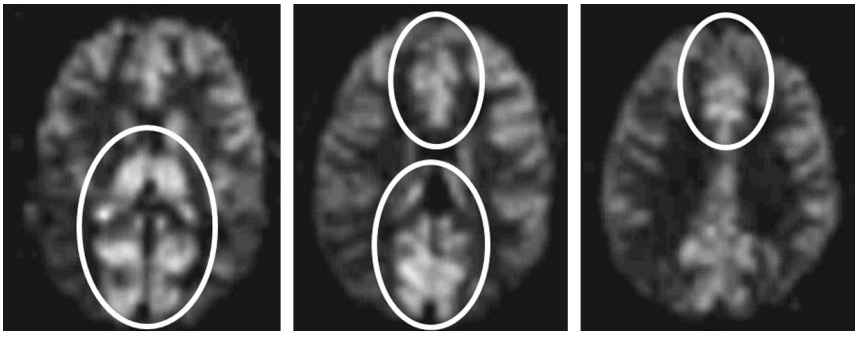

Figure 7. Zones of physiological hyperperfusion. These perfusion-weighted images, in three different subjects, show the internal bilateral occipital and frontal physiological hyperperfusion (circles).

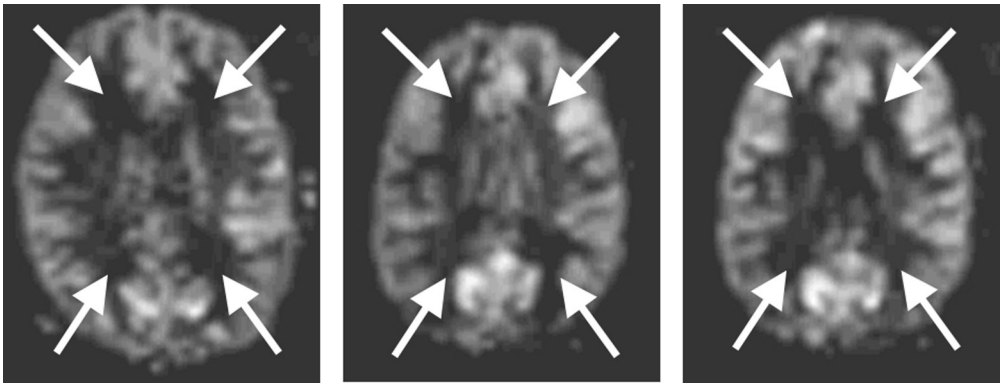

Figure 8. Zones of physiological hypoperfusion. These perfusion-weighted images, in three different subjects, obtained with pulsed labeling, show the physiological hypoperfusion of the junctional territories (arrows).

Post-gadolinium arterial spin labeling

Gadolinium contrast media significantly reduce the T1 of the blood. This shortening is such that, after labeling by ASL, it is not possible to detect the minor difference between the labeled and control images (Fig. 9).

Therefore, it is not possible to carry out an ASL sequence immediately after the injection of gadolinium. A minimum of 12 hours seems necessary with respect to the half-life of gadolinium contrast media.

Non-specific artifacts

A certain number of artifacts are not ASL specific, but have an effect on the quality and homogeneity of the mapping.

Magnetic susceptibility artifacts

Magnetic susceptibility artifacts are related to the rapid acquisition of images and are particularly visible with EPI sequences. They are visible as a focal reduction in perfusion

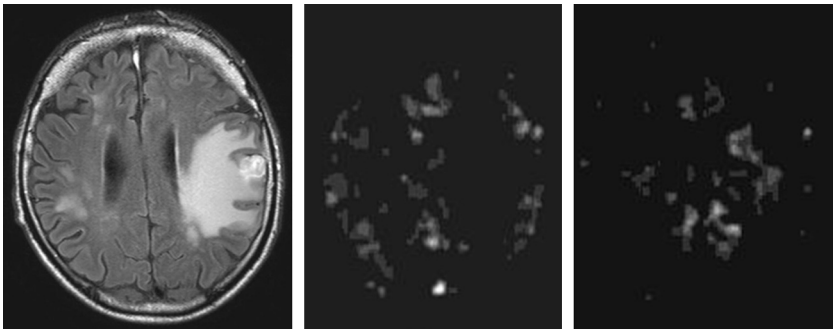

Figure 9. Arterial spin labeling after the injection of gadolinium. The arterial spin labeling mapping obtained after the injection of gadolinium are not analysable, as in this case of secondary left parietal localization.

at the base of the skull, in the temporal and frontal region (Fig. 10). They are also present in hematomas, calcifications, metal materials or in contact with early post-surgical changes.

One way to reduce these artifacts is to use less sensitive methods of image acquisition such as True-FISP or 3D GRASE and/or use parallel imaging [20,25,27,45].

Movement artifacts

The multiple repetitions required to obtain a satisfactory SNR make the sequence sensitive to movement artifacts. As in BOLD-fMRI, these artifacts may also produce strips at the periphery of the brain (Fig. 11) [41]. These artifacts may be the source of focal or diffuse areas of false hypo or hyperperfusion (Fig. 12). The methods of adjustment are of limited efficacy when the movements are sudden. It is therefore preferable to exclude from the analysis all images overly subject to movement.

Sensitivity of the coil elements

The sensitivity of the different elements in a phase array coil differs slightly. If an element is defective or if the sensitivity differs greatly from the other elements, this results in a peripheral focal area where the perfusion differs (Fig. 13). It is necessary to confirm this artifact by obtaining a second sequence acquisition by positioning the patient's head differently in the coil. A post-treatment correction may also be added by using M_0 mapping [41].

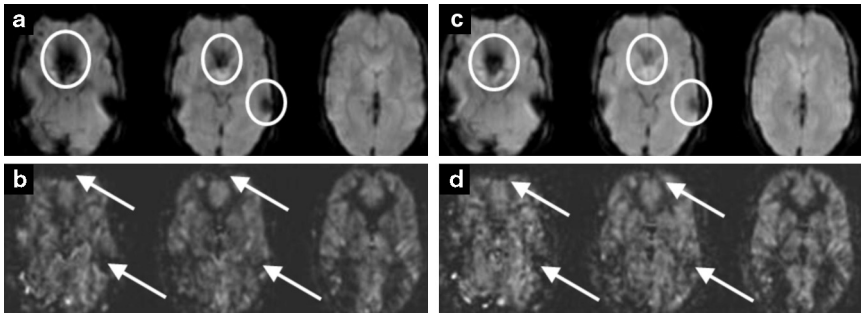

Figure 10. Artifacts of magnetic susceptibility. a: the artifacts of magnetic susceptibility are clearly visible (circles) on the native images; b: on the cerebral blood flow mapping, they are visible in the form of a focal reduction in perfusion; c—d: the same images acquired after the application of parallel imaging (GRAPPA with a factor 2), reveal a reduction in these artifacts on the native images (c) as well as on the CBF mapping (d).

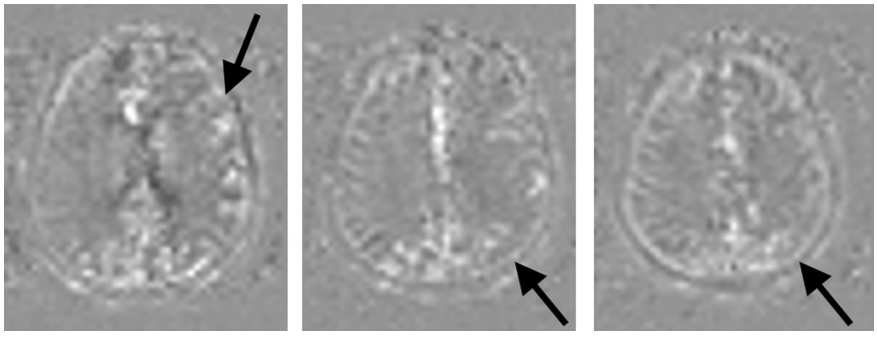

Figure 11. Movement artifacts. The concentric circular images in hypo- and hypersignal around the brain (arrows) attest to the presence of movement artifacts.

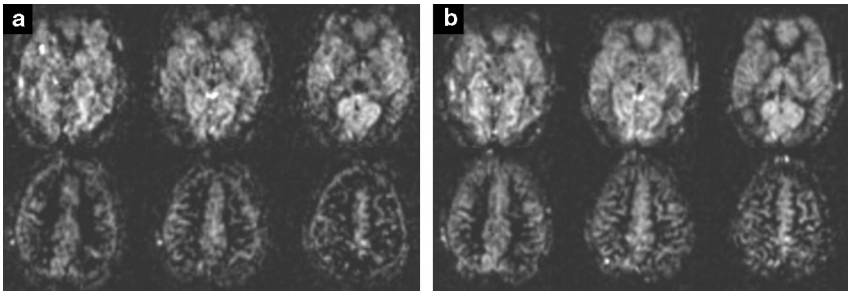

Figure 12. Movement artifacts. a—b: if the patient moves during the acquisition, the mapping appears more noised with a globally weaker signal (a), when compared with the images acquired without movement (b).

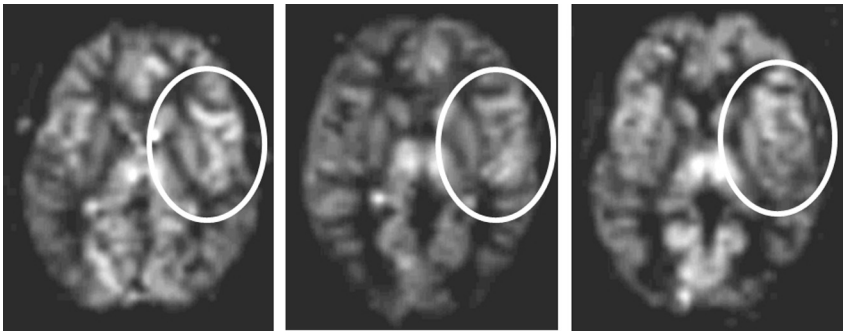

Figure 13. Sensitivity of a phase array coil element. These perfusion-weighted images, in three subjects, acquired with the same coil, show that the signal appears greater in all subjects when near one of the coil elements.

Parallel imaging artifacts

These non-specific artifacts are less distinct on perfusion mapping than on the native imaging, due to the subtraction [25]. With the SENSE and mSENSE techniques, these artifacts appear as aliasing [46]. With the GRAPPA technique, these artifacts produce a diffuse or even grainy image with high acceleration factors (Fig. 14) [27].

Clinical applications

Cerebral perfusion

ASL has been applied in most of the neuroscience fields, on healthy subjects and patients, thanks to its non-invasive nature and the access to a reproducible and validated quantification of the CBF with respect to other cerebral perfusion

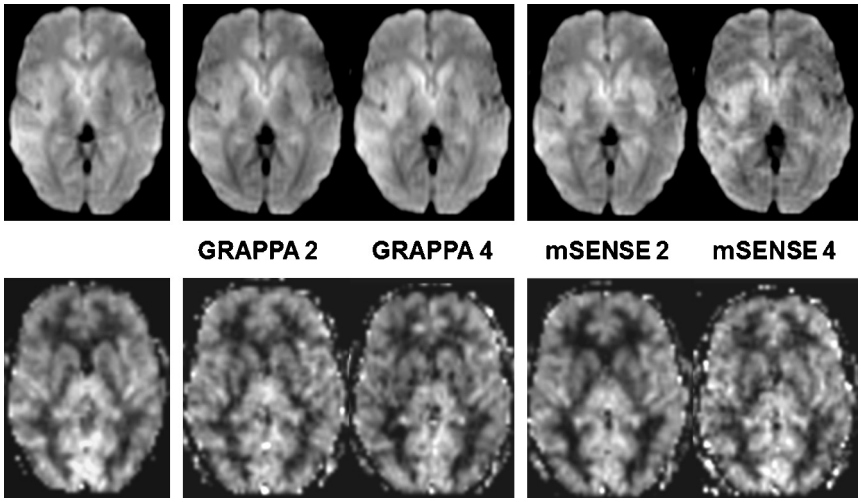

Figure 14. Parallel imaging artifacts. Parallel imaging artifacts are above all visible in the native images (upper line). They increase with the parallel imaging factor (here factor 2 and 4). With the generalized autocalibrating partially parallel acquisitions (GRAPPA) technique, they are the cause of a grainy appearance of the image, while with the sensitivity encoding technique (SENSE), they provide aliasing. On the cerebral blood flow mapping (lower line), they are less clearly visible, but are responsible for an increase in noise.

techniques [38,47]. Several recent reviews have described these applications [35,48,49].

The value of ASL has been demonstrated in acute and chronic neurovascular diseases where the perfusion anomalies revealed concord with other techniques (Fig. 15) [50—52], sometimes with an overestimate when compared with perfusion MRI [53]. In tumor disorders, ASL specifies the grade of the tumor and measures the effects of antiangiogenic therapy [54—56]. Local changes in cerebral perfusion have also been detected in epilepsy and neurodegenerative disease, such as Alzheimer's disease or frontotemporal dementia [55,57]. The latter two disorders can even be distinguished by ASL with their different profiles of perfusional abnormalities [58]. In amyotrophic lateral sclerosis, the reduction in perfusion is correlated with the severity of the disease [59]. Several rare studies have examined psychiatric diseases, in particular depression [60,61], sleep deprivation [62], or the addictions [63]. Certain disorders, such as multiple sclerosis, have been very little studied by ASL [64]. Finally, in spite of the advantages of ASL in the pediatric population, in particular a shorter transit time and a higher CBF than in the adult, very little specific works has been carried out on this population [65—67].

If ASL in general analyses the overall cerebral tissue perfusion, selective labeling methods of a cervical artery also analyze the perfusion of the downstream area and the presence of possible substitutes for this area via the development of collaterality [16,68].

Functional MRI with arterial spin labeling (fASL)

It is possible to obtain mapping of brain activation by the analysis of the time course of the perfusion measured by ASL during an activation paradigm (fASL) and by directly studying the variations in perfusion that accompany neuronal activation. A recent review has described this technique and its applications [69].

fASL paradigms have explored motor, visual and language functions [70—73]. fASL has also explored the mechanisms of learning and memorization [74], stress control [75] or pain response [76]. The main interest over the BOLD-fMRI is the absolute quantification of CBF variations during neuronal activation [70,77]. Several recent studies have shown that fASL benefits from better inter-individual [72] and intra-individual [71] reproducibility. fASL also seems to be more precise than BOLD-fMRI in terms of temporal resolution, with a more synchronous signal kinetics of neuronal activation [77]. Finally, fASL provides a better spatial localization of neuron activity [73].

Extra-cerebral applications of arterial spin labeling

From the beginning, ASL was used to study renal perfusion [78]. The measurements, mainly obtained with FAIR techniques, are correlated with those obtained by SPECT, including cases of stenosis of the renal artery, and are similar in the renal cortex to those with T1-weighted perfusion MRI [79,80]. A recent study has demonstrated the good intra- and inter-session reproducibility of these measurements [81]. The feasibility of ASL for the characterization of renal adenocarcinomas and their monitoring after ablation by radiofrequency has been demonstrated [82,83].

With the technical developments, it seems possible to obtain, within an experimental context, information about the perfusion of pathological bone or the pancreas, or even an organ with a low perfusion level, such as the prostate [84—86].

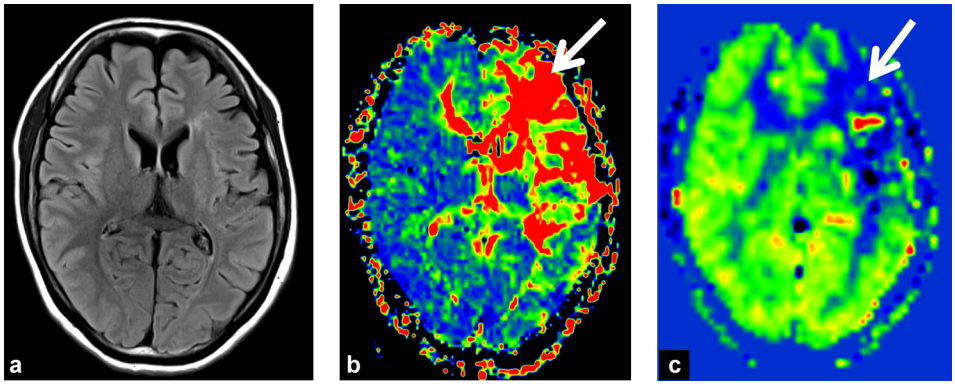

Figure 15. Chronic thrombosis of the internal left carotid artery. a: the FLAIR axial section reveals a small ischemic sequela of deep frontal left white matter; b: the T2*-weighted perfusion sequence of magnetic susceptibility, with the injection of gadolinium, demonstrates an increase in the mean transit time in the anterior part of the territory of the left middle cerebral artery (arrow); c: a superimposable perfusion anomaly is also visible on the mapping of the arterial blood slow of the arterial spin labeling.

Conclusion

The absence of irradiation or the exogenous injection of a contrast medium, as well as the access to a reproducible quantification of perfusion parameters, make ASL an especially interesting technique in the study of tissue perfusion, in particular the brain and kidney. ASL is becoming available on clinical MRI and its use is increasingly easy. Nevertheless, the quality of ASL images may be limited by their low signal-noise ratio and by several types of artifacts that are important to know. In addition, homogenization of the techniques of proton labeling, image acquisition and data processing will allow for the large-scale use of ASL and thereby validate its potential clinical applications.

TAKE-HOME MESSAGES

Advantages of ASL
- No irradiation
- No injection of exogenous contrast medium
- Absolute quantification possible of the tissue blood flow and the arterial transit time
- Repeated measurements possible
- Reproducibility

Disadvantages of ASL
- Low signal-noise ratio
- Minimum acquisition time: 3 min
- Limited spatial resolution
- Quantification of the tissue blood volume impossible (ex: cerebral blood volume)
- Absence of harmonization of techniques (type of labeling, image acquisition, post-treatment) between the manufacturers
- Post-treatment optimization, automation and standardization still in development

Clinical case

This 55-year-old woman presents a left parietal expansive process (Fig. 16). The T1 post-contrast axial section reveals annular enhancement (a). An increase in the cerebral blood volume is visible (white arrow) on the mapping calculated from the magnetic susceptibility of gadolinium in a T2*-weighted perfusion sequence (b). The perfusion mapping obtained by ASL before the injection of gadolinium (c) also shows this hyperperfusion in a ring (black arrow). The diagnosis of glioblastoma is made after examination of the surgical sample taken after the MRI.

Questions

1. What is the main perfusion parameter measured by ASL? What are the characteristics?
2. What are the main advantages and disadvantages of ASL?
3. Why is the use of a 3 T MRI also an advantage for ASL?

Answers

1. The CBF. It represents the amount of blood that passes through the tissue per unit of time. The unit is mL/100 g/min. The quantification of the CBF by ASL is reliable, reproducible and correlated with other techniques, in particular the techniques of nuclear medicine. By using multi-TI techniques, that are still not available on clinical MRI, it's possible to obtain measurements of the arterial transit time. However, the measurement of the cerebral blood volume is not possible with ASL.
2. Provided that the usual contra-indications are complied with for MRI, ASL is a completely non-invasive technique to study perfusion (no ionizing radiation, no exogenous injection of contrast media). The absolute quantification of the CBF is possible and is reliable and reproducible. The main disadvantage is the low signal-noise ratio related to the subtraction between ''labeled'' images and ''control'' images. This requires a minimum acquisition of 3 min and a spatial resolution that is inferior that of the other techniques (MRI or CT-scan). The multiplicity of acquisition techniques and processing currently available on clinical MRI render large-scale use difficult.

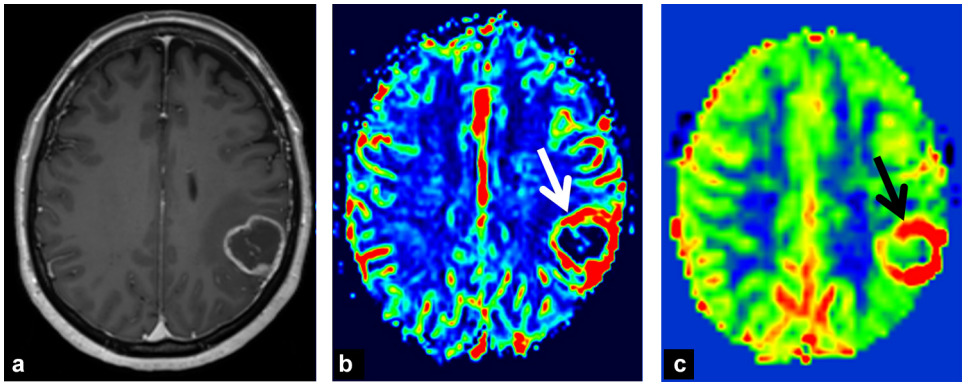

Figure 16. The T1 post-contrast axial slice shows annular contrast (a). An increase in the cerebral blood volume is visible (b, white arrow) on the mapping calculated from the T2*-weighted perfusion sequence of magnetic susceptibility with the injection of gadolinium (b). The perfusion mapping obtained by arterial spin labeling before the injection of gadolinium (c) also shows this hyperperfusion in ring (black arrow).

3. The increase in the magnetic field increases the signal-noise ratio. Moreover, since the relaxation time is longer, the duration of the labeling increases. The increase in distortions is widely compensated at the encephalic level by the use of phased array coils (the signal increases with the number of elements, near the elements, as well as at the center of the image) and by the use of parallel imaging.

Disclosure of interest

The authors declare that they have no conflicts of interest concerning this article.

Acknowledgements

This work was carried out with the support of Société française de radiologie (2011 Research Grant) and Société française de neuroradiologie (2010 Mobility Grant).

References

[1] Detre JA, Leigh JS, Williams DS, Koretsky AP. Perfusion imaging. Magn Reson Med 1992;23:37—45.
[2] Williams DS, Detre JA, Leigh JS, Koretsky AP. Magnetic resonance imaging of perfusion using spin inversion of arterial water. Proc Natl Acad Sci U S A 1992;89:212—6.
[3] Wang J, Alsop DC, Li L, Listerud J, Gonzalez-At JB, Schnall MD, et al. Comparison of quantitative perfusion imaging using arterial spin labeling at 1.5 and 4.0 Tesla. Magn Reson Med 2002;48:242—54.
[4] Alsop DC, Detre JA. Multisection cerebral blood flow MR imaging with continuous arterial spin labeling. Radiology 1998;208:410—6.
[5] Zaharchuk G, Ledden PJ, Kwong KK, Reese TG, Rosen BR, Wald LL. Multislice perfusion and perfusion territory imaging in humans with separate label and image coils. Magn Reson Med 1999;41:1093—8.
[6] Zhang W, Silva AC, Williams DS, Koretsky AP. NMR measurement of perfusion using arterial spin labeling without saturation of macromolecular spins. Magn Reson Med 1995;33:370—6.
[7] Silva AC, Kim SG. Pseudo-continuous arterial spin labeling technique for measuring CBF dynamics with high temporal resolution. Magn Reson Med 1999;42:425—9.
[8] Golay X, Hendrikse J, Lim TC. Perfusion imaging using arterial spin labeling. Top Magn Reson Imaging 2004;15:10—27.
[9] Kim SG. Quantification of relative cerebral blood flow change by flow-sensitive alternating inversion recovery (FAIR) technique: application to functional mapping. Magn Reson Med 1995;34:293—301.
[10] Edelman RR, Siewert B, Darby DG, Thangaraj V, Nobre AC, Mesulam MM, et al. Qualitative mapping of cerebral blood flow and functional localization with echo-planar MR imaging and signal targeting with alternating radio frequency. Radiology 1994;192:513—20.
[11] Edelman RR, Chen Q. EPISTAR MRI: multislice mapping of cerebral blood flow. Magn Reson Med 1998;40:800—5.
[12] Golay X, Stuber M, Pruessmann KP, Meier D, Boesiger P. Transfer insensitive labeling technique (TILT): application to multislice functional perfusion imaging. J Magn Reson Imaging 1999;9:454—61.
[13] Wong EC, Buxton RB, Frank LR. Implementation of quantitative perfusion imaging techniques for functional brain mapping using pulsed arterial spin labeling. NMR Biomed 1997;10:237—49.
[14] Luh WM, Wong EC, Bandettini PA, Hyde JS. QUIPSS II with thin-slice TI1 periodic saturation: a method for improving accuracy of quantitative perfusion imaging using pulsed arterial spin labeling. Magn Reson Med 1999;41:1246—54.
[15] Wong EC, Buxton RB, Frank LR. Quantitative imaging of perfusion using a single subtraction (QUIPSS and QUIPSS II). Magn Reson Med 1998;39:702—8.
[16] Hendrikse J, van der Grond J, Lu H, van Zijl PC, Golay X. Flow territory mapping of the cerebral arteries with regional perfusion MRI. Stroke 2004;35:882—7.
[17] Golay X, Petersen ET, Hui F. Pulsed star labeling of arterial regions (PULSAR): a robust regional perfusion technique for high field imaging. Magn Reson Med 2005;53:15—21.
[18] Werner R, Norris DG, Alfke K, Mehdorn HM, Jansen O. Continuous artery-selective spin labeling (CASSL). Magn Reson Med 2005;53:1006—12.
[19] Wong EC, Cronin M, Wu WC, Inglis B, Frank LR, Liu TT. Velocity-selective arterial spin labeling. Magn Reson Med 2006;55:1334—41.
[20] Fernandez-Seara MA, Wang Z, Wang J, Rao HY, Guenther M, Feinberg DA, et al. Continuous arterial spin labeling perfusion measurements using single shot 3D GRASE at 3 T. Magn Reson Med 2005;54:1241—7.
[21] Ye FQ, Frank JA, Weinberger DR, McLaughlin AC. Noise reduction in 3D perfusion imaging by attenuating the static signal in arterial spin tagging (ASSIST). Magn Reson Med 2000;44:92—100.
[22] Golay X, Petersen ET. Arterial spin labeling: benefits and pitfalls of high magnetic field. Neuroimaging Clin N Am 2006;16:259—68 [x].
[23] Wang J, Zhang Y, Wolf RL, Roc AC, Alsop DC, Detre JA. Amplitude-modulated continuous arterial spin-labeling 3.0-T perfusion MR imaging with a single coil: feasibility study. Radiology 2005;235:218—28.
[24] de Zwart JA, Ledden PJ, Kellman P, van Gelderen P, Duyn JH. Design of a SENSE-optimized high-sensitivity MRI receive coil for brain imaging. Magn Reson Med 2002;47:1218—27.
[25] Wang Z, Wang J, Connick TJ, Wetmore GS, Detre JA. Continuous ASL (CASL) perfusion MRI with an array coil and parallel imaging at 3 T. Magn Reson Med 2005;54:732—7.
[26] de Zwart JA, Ledden PJ, van Gelderen P, Bodurka J, Chu R, Duyn JH. Signal-to-noise ratio and parallel imaging performance of a 16-channel receive-only brain coil array at 3.0 Tesla. Magn Reson Med 2004;51:22—6.
[27] Ferré JC, Petr J, Bannier E, Barillot C, Gauvrit JY. Improving quality of arterial spin labeling MR imaging at 3 tesla with a 32-channel coil and parallel imaging. J Magn Reson Imaging 2012;35:1233—9.
[28] Lupo JM, Lee MC, Han ET, Cha S, Chang SM, Berger MS, et al. Feasibility of dynamic susceptibility contrast perfusion MR imaging at 3 T using a standard quadrature head coil and eight-channel phased-array coil with and without SENSE reconstruction. J Magn Reson Imaging 2006;24:520—9.
[29] Wang Z, Aguirre GK, Rao H, Wang J, Fernandez-Seara MA, Childress AR, et al. Empirical optimization of ASL data analysis using an ASL data processing toolbox: ASLtbx. Magn Reson Imaging 2008;26:261—9.
[30] Frouin F, Duteil S, Lesage D, Carlier PG, Herment A, Leroy-Willig A. An automated image-processing strategy to analyze dynamic arterial spin labeling perfusion studies. Application to human skeletal muscle under stress. Magn Reson Imaging 2006;24:941—51.
[31] Chappell MA, MacIntosh BJ, Donahue MJ, Gunther M, Jezzard P, Woolrich MW. Separation of macrovascular signal in multi-inversion time arterial spin labelling MRI. Magn Reson Med 2010;63:1357—65.

[32] Asllani I, Borogovac A, Brown TR. Regression algorithm correcting for partial volume effects in arterial spin labeling MRI. Magn Reson Med 2008;60:1362—71.
[33] Wells JA, Thomas DL, King MD, Connelly A, Lythgoe MF, Calamante F. Reduction of errors in ASL cerebral perfusion and arterial transit time maps using image de-noising. Magn Reson Med 2010;64:715—24.
[34] Buxton RB, Frank LR, Wong EC, Siewert B, Warach S, Edelman RR. A general kinetic model for quantitative perfusion imaging with arterial spin labeling. Magn Reson Med 1998;40:383—96.
[35] Petersen ET, Zimine I, Ho YC, Golay X. Non-invasive measurement of perfusion: a critical review of arterial spin labelling techniques. Br J Radiol 2006;79:688—701.
[36] Petersen ET, Lim T, Golay X. Model-free arterial spin labeling quantification approach for perfusion MRI. Magn Reson Med 2006;55:219—32.
[37] Zaharchuk G, Do HM, Marks MP, Rosenberg J, Moseley ME, Steinberg GK. Arterial spin-labeling MRI can identify the presence and intensity of collateral perfusion in patients with moyamoya disease. Stroke 2011;42:2485—91.
[38] Petersen ET, Mouridsen K, Golay X. The QUASAR reproducibility study, part II: results from a multi-center Arterial Spin Labeling test-retest study. Neuroimage 2010;49:104—13.
[39] Ye FQ, Mattay VS, Jezzard P, Frank JA, Weinberger DR, McLaughlin AC. Correction for vascular artifacts in cerebral blood flow values measured by using arterial spin tagging techniques. Magn Reson Med 1997;37:226—35.
[40] Cavusoglu M, Pfeuffer J, Ugurbil K, Uludag K. Comparison of pulsed arterial spin labeling encoding schemes and absolute perfusion quantification. Magn Reson Imaging 2009;27:1039—45.
[41] Deibler AR, Pollock JM, Kraft RA, Tan H, Burdette JH, Maldjian JA. Arterial spin-labeling in routine clinical practice, part 1: technique and artifacts. AJNR Am J Neuroradiol 2008;29:1228—34.
[42] Mamo H, Meric P, Luft A, Seylaz J. Hyperfrontal pattern of human cerebral circulation. Variations with age and atherosclerotic state. Arch Neurol 1983;40:626—32.
[43] Hendrikse J, Petersen ET, van Laar PJ, Golay X. Cerebral border zones between distal end branches of intracranial arteries: MR imaging. Radiology 2008;246:572—80.
[44] van Osch MJ, Teeuwisse WM, van Walderveen MA, Hendrikse J, Kies DA, van Buchem MA. Can arterial spin labeling detect white matter perfusion signal? Magn Reson Med 2009;62:165—73.
[45] Boss A, Martirosian P, Klose U, Nagele T, Claussen CD, Schick F. FAIR-TrueFISP imaging of cerebral perfusion in areas of high magnetic susceptibility differences at 1.5 and 3 Tesla. J Magn Reson Imaging 2007;25:924—31.
[46] Preibisch C, Wallenhorst T, Heidemann R, Zanella FE, Lanfermann H. Comparison of parallel acquisition techniques generalized autocalibrating partially parallel acquisitions (GRAPPA) and modified sensitivity encoding (mSENSE) in functional MRI (fMRI) at 3 T. J Magn Reson Imaging 2008;27:590—8.
[47] Wang Y, Saykin AJ, Pfeuffer J, Lin C, Mosier KM, Shen L, et al. Regional reproducibility of pulsed arterial spin labeling perfusion imaging at 3 T. Neuroimage 2011;54:1188—95.
[48] Detre JA, Rao H, Wang DJ, Chen YF, Wang Z. Applications of arterial spin labeled MRI in the brain. J Magn Reson Imaging 2012;35:1026—37.
[49] Wolf RL, Detre JA. Clinical neuroimaging using arterial spin-labeled perfusion magnetic resonance imaging. Neurotherapeutics 2007;4:346—59.
[50] Bokkers RP, van Osch MJ, van der Worp HB, de Borst GJ, Mali WP, Hendrikse J. Symptomatic carotid artery stenosis: impairment of cerebral autoregulation measured at the brain tissue level with arterial spin-labeling MR imaging. Radiology 2010;256:201—8.
[51] Siewert B, Schlaug G, Edelman RR, Warach S. Comparison of EPISTAR and T2*-weighted gadolinium-enhanced perfusion imaging in patients with acute cerebral ischemia. Neurology 1997;48:673—9.
[52] Wang DJ, Alger JR, Qiao JX, Hao Q, Hou S, Fiaz R, et al. The value of arterial spin-labeled perfusion imaging in acute ischemic stroke: comparison with dynamic susceptibility contrast-enhanced MRI. Stroke 2012;43:1018—24.
[53] Zaharchuk G, El Mogy IS, Fischbein NJ, Albers GW. Comparison of arterial spin labeling and bolus perfusion-weighted imaging for detecting mismatch in acute stroke. Stroke 2012;43:1843—8.
[54] Tourdias T, Rodrigo S, Oppenheim C, Naggara O, Varlet P, Amoussa S, et al. Pulsed arterial spin labeling applications in brain tumors: practical review. J Neuroradiol 2008;35:79—89.
[55] Noguchi T, Yoshiura T, Hiwatashi A, Togao O, Yamashita K, Nagao E, et al. Perfusion imaging of brain tumors using arterial spin-labeling: correlation with histopathologic vascular density. AJNR Am J Neuroradiol 2008;29:688—93.
[56] Weber MA, Zoubaa S, Schlieter M, Juttler E, Huttner HB, Geletneky K, et al. Diagnostic performance of spectroscopic and perfusion MRI for distinction of brain tumors. Neurology 2006;66:1899—906.
[57] Du AT, Jahng GH, Hayasaka S, Kramer JH, Rosen HJ, Gorno-Tempini ML, et al. Hypoperfusion in frontotemporal dementia and Alzheimer disease by arterial spin labeling MRI. Neurology 2006;67:1215—20.
[58] Hu WT, Wang Z, Lee VM, Trojanowski JQ, Detre JA, Grossman M. Distinct cerebral perfusion patterns in FTLD and AD. Neurology 2010;75:881—8.
[59] Rule RR, Schuff N, Miller RG, Weiner MW. Gray matter perfusion correlates with disease severity in ALS. Neurology 2010;74:821—7.
[60] Lui S, Parkes LM, Huang X, Zou K, Chan RC, Yang H, et al. Depressive disorders: focally altered cerebral perfusion measured with arterial spin-labeling MR imaging. Radiology 2009;251:476—84.
[61] Duhameau B, Ferre JC, Jannin P, Gauvrit JY, Verin M, Millet B, et al. Chronic and treatment-resistant depression: a study using arterial spin labeling perfusion MRI at 3 Tesla. Psychiatry Res 2010;182:111—6.
[62] Clark CP, Brown GG, Frank L, Thomas L, Sutherland AN, Gillin JC. Improved anatomic delineation of the antidepressant response to partial sleep deprivation in medial frontal cortex using perfusion-weighted functional MRI. Psychiatry Res 2006;146:213—22.
[63] Franklin TR, Wang Z, Wang J, Sciortino N, Harper D, Li Y, et al. Limbic activation to cigarette smoking cues independent of nicotine withdrawal: a perfusion fMRI study. Neuropsychopharmacology 2007;32:2301—9.
[64] Rashid W, Parkes LM, Ingle GT, Chard DT, Toosy AT, Altmann DR, et al. Abnormalities of cerebral perfusion in multiple sclerosis. J Neurol Neurosurg Psychiatry 2004;75:1288—93.
[65] Chen J, Licht DJ, Smith SE, Agner SC, Mason S, Wang S, et al. Arterial spin labeling perfusion MRI in pediatric arterial ischemic stroke: initial experiences. J Magn Reson Imaging 2009;29:282—90.
[66] Oguz KK, Golay X, Pizzini FB, Freer CA, Winrow N, Ichord R, et al. Sickle cell disease: continuous arterial spin-labeling perfusion MR imaging in children. Radiology 2003;227:567—74.
[67] Wang J, Licht DJ, Jahng GH, Liu CS, Rubin JT, Haselgrove J, et al. Pediatric perfusion imaging using pulsed arterial spin labeling. J Magn Reson Imaging 2003;18:404—13.
[68] van Laar PJ, van der Grond J, Hendrikse J. Brain perfusion territory imaging: methods and clinical applications of selective arterial spin-labeling MR imaging. Radiology 2008;246:354—64.

[69] Raoult H, Gauvrit JY, Petr J, Bannier E, Le Rumeur E, Barillot C, et al. Innovations in functional MR imaging of the brain: arterial spin labeling and diffusion. J Radiol 2011;92:878—88.
[70] Ances BM, Leontiev O, Perthen JE, Liang C, Lansing AE, Buxton RB. Regional differences in the coupling of cerebral blood flow and oxygen metabolism changes in response to activation: implications for BOLD-fMRI. Neuroimage 2008;39:1510—21.
[71] Leontiev O, Buxton RB. Reproducibility of BOLD, perfusion, and CMRO2 measurements with calibrated-BOLD fMRI. Neuroimage 2007;35:175—84.
[72] Wang J, Aguirre GK, Kimberg DY, Roc AC, Li L, Detre JA. Arterial spin labeling perfusion fMRI with very low task frequency. Magn Reson Med 2003;49:796—802.
[73] Raoult H, Petr J, Bannier E, Stamm A, Gauvrit JY, Barillot C, et al. Arterial spin labeling for motor activation mapping at 3 T with a 32-channel coil: reproducibility and spatial accuracy in comparison with BOLD fMRI. Neuroimage 2011;58:157—67.
[74] Fernandez-Seara MA, Aznarez-Sanado M, Mengual E, Loayza FR, Pastor MA. Continuous performance of a novel motor sequence leads to highly correlated striatal and hippocampal perfusion increases. Neuroimage 2009;47:1797—808.
[75] Wang J, Rao H, Wetmore GS, Furlan PM, Korczykowski M, Dinges DF, et al. Perfusion functional MRI reveals cerebral blood flow pattern under psychological stress. Proc Natl Acad Sci U S A 2005;102:17804—9.
[76] Owen DG, Bureau Y, Thomas AW, Prato FS, St Lawrence KS. Quantification of pain-induced changes in cerebral blood flow by perfusion MRI. Pain 2008;136:85—96.
[77] Obata T, Liu TT, Miller KL, Luh WM, Wong EC, Frank LR, et al. Discrepancies between BOLD and flow dynamics in primary and supplementary motor areas: application of the balloon model to the interpretation of BOLD transients. Neuroimage 2004;21:144—53.
[78] Roberts DA, Detre JA, Bolinger L, Insko EK, Lenkinski RE, Pentecost MJ, et al. Renal perfusion in humans: MR imaging with spin tagging of arterial water. Radiology 1995;196:281—6.
[79] Fenchel M, Martirosian P, Langanke J, Giersch J, Miller S, Stauder NI, et al. Perfusion MR imaging with FAIR true FISP spin labeling in patients with and without renal artery stenosis: initial experience. Radiology 2006;238:1013—21.
[80] Winter JD, St Lawrence KS, Margaret Cheng HL. Quantification of renal perfusion: comparison of arterial spin labeling and dynamic contrast-enhanced MRI. J Magn Reson Imaging 2011;34(3):608—15.
[81] Cutajar M, Thomas DL, Banks T, Clark CA, Golay X, Gordon I. Repeatability of renal arterial spin labelling MRI in healthy subjects. Magma 2012;25:145—53.
[82] Boss A, Martirosian P, Schraml C, Clasen S, Fenchel M, Anastasiadis A, et al. Morphological, contrast-enhanced and spin labeling perfusion imaging for monitoring of relapse after RF ablation of renal cell carcinomas. Eur Radiol 2006;16:1226—36.
[83] De Bazelaire C, Rofsky NM, Duhamel G, Michaelson MD, George D, Alsop DC. Arterial spin labeling blood flow magnetic resonance imaging for the characterization of metastatic renal cell carcinoma(1). Acad Radiol 2005;12:347—57.
[84] Li X, Metzger GJ. Feasibility of measurement of prostate perfusion with arterial spin labeling. NMR Biomed 2013;26(1): 51—7.
[85] Schraml C, Schwenzer NF, Martirosian P, Claussen CD, Schick F. Perfusion imaging of the pancreas using an arterial spin labeling technique. J Magn Reson Imaging 2008;28:1459—65.
[86] Fenchel M, Konaktchieva M, Weisel K, Kraus S, Brodoefel H, Claussen CD, et al. Early response assessment in patients with multiple myeloma during anti-angiogenic therapy using arterial spin labelling: first clinical results. Eur Radiol 2010;20:2899—906.